

# Critical Evaluation of Jet-A Spray Combustion Using Propane Chemical Kinetics in Gas Turbine Combustion Simulated by KIVA-II

H.L. Nguyen  
*Lewis Research Center  
Cleveland, Ohio*

and

S.-J. (Benjamin) Ying  
*University of South Florida  
Tampa, Florida*

Prepared for the  
26th Joint Propulsion Conference  
cosponsored by the AIAA, SAE, ASME, and ASEE  
Orlando, Florida, July 16-18, 1990



(NASA-TM-103173) CRITICAL EVALUATION OF  
JET-A SPRAY COMBUSTION USING PROPANE  
CHEMICAL KINETICS IN GAS TURBINE COMBUSTION  
SIMULATED BY KIVA-II (NASA) 21 p USCL 21B

N90-26170

03/31 0295176  
Unclass



CRITICAL EVALUATION OF JET-A SPRAY COMBUSTION USING PROPANE CHEMICAL  
KINETICS IN GAS TURBINE COMBUSTION SIMULATED BY KIVA-II

H.L. Nguyen  
National Aeronautics and Space Administration  
Lewis Research Center  
Cleveland, Ohio 44135

and

S.-J. (Benjamin) Ying  
University of South Florida  
Tampa, Florida 33620

SUMMARY

Jet-A spray combustion has been evaluated in gas turbine combustion with the use of propane chemical kinetics as the first approximation for the chemical reactions. In this work, the numerical solutions are obtained by using the KIVA-II computer code. The KIVA-II code is the most developed of the available multidimensional combustion computer programs for application of the in-cylinder combustion dynamics of internal combustion engines. The released version of KIVA-II assumes that 12 chemical species are present; the code uses an Arrhenius kinetic-controlled combustion model governed by a four-step global chemical reaction and six equilibrium reactions. Our efforts involve the addition of Jet-A thermophysical properties and the implementation of detailed reaction mechanisms for propane oxidation. Three different detailed reaction mechanism models are considered. The first model consists of 131 reactions and 45 species. This is considered as the full mechanism which is developed through the study of chemical kinetics of propane combustion in an enclosed chamber. The full mechanism is evaluated by comparing calculated ignition delay times with available shock tube data. However, these detailed reactions occupy too much computer memory and CPU time for the computation. Therefore, it only serves as a benchmark case by which to evaluate other simplified models.

Two possible simplified models have been tested in the existing computer code KIVA-II for the same conditions as used with the full mechanism. One model is obtained through a sensitivity analysis using LSENS, the general kinetics and sensitivity analysis program code of D.A. Bittker and K. Radhakrishnan. This model consists of 45 chemical reactions and 27 species. The other model is based on the work published by C.K. Westbrook and F.L. Dryer. This simplified model consists of 5 chemical reactions and 12 species. The numerical results indicate that the variation of the maximum flame temperature is within 20 percent as compared with that of the full mechanism of 131 reactions. The chemical compositions of major components such as  $C_3H_8$ ,  $H_2O$ ,  $O_2$ ,  $CO_2$ , and  $N_2$  are of the same order of magnitude. However, the concentrations of pollutants are quite different. Details are presented later in this paper.

## INTRODUCTION

The goal of gas turbine combustion system design and development is to meet many mutually conflicting trade-offs between high combustion efficiency over a wide operating envelope and low  $\text{NO}_x$  emissions: low smoke, low lean flame stability limits, and good starting characteristics; and low combustion system pressure loss, low pattern factor, and high structural durability. Recent advances in high-speed and large-memory computers, numerical algorithms, grid generation, and combustion modeling have a powerful positive influence on future design capability. To accurately model combustion system subcomponents, significant improvements in physical modeling and numerical techniques are required.

In this work, a detailed chemical kinetics mechanism of a simple hydrocarbon, such as propane, is used to predict combustion flows and emissions of typical combustion systems representative of gas turbine combustors using multidimensional codes. Previous multidimensional computations of combustion and flow characteristics of gas turbine combustor sector or subcomponents used global or quasi-global chemical kinetics mechanisms. These combustion models may be able to predict qualitatively the average value of heat release; however, they are unable to predict local chemical equilibrium and detailed combustion species profiles, including  $\text{NO}_x$  emission. In the current work, the fuel used is Jet-A, whose physical properties are known and are given later in this paper. However, the chemical kinetics for Jet-A combustion with air are not presently available. It is necessary to use the propane chemical kinetics for the simulation of Jet-A combustion as a first step approximation. However, even the chemical kinetics for propane are not well understood. In this work, the propane oxidation mechanisms consisting of 131 reactions (ref. 1) are used to perform benchmark computations and serve to evaluate the other two reduced mechanisms.

The numerical simulation is done by using the code KIVA-II, which was originally designed for the simulation of turbulent reactive flows in piston engines. The code is modified for testing propane chemical kinetics in two-dimensional gas turbine combustion. The purpose of using the KIVA-II code is that it is considered to be very well developed and represents present state-of-the-art. A description of KIVA-II and its modifications will follow.

## DESCRIPTION OF COMPUTER CODE KIVA-II

The computer code KIVA-II was originally designed to simulate numerically transient two- and three-dimensional reactive fluid flows with sprays in piston engines. The dynamics and evaporation of spray droplets, spark ignition, the chemical kinetics of combustion, turbulence, and the boundary effects of the flow near the walls are considered in detail. Turbulence is modeled by using two-equation  $k-\epsilon$  model equations and an implicit-continuous Eulerian (ICE) technique is used for the flow solver. A stochastic particle method is used to calculate the evaporation rate of liquid sprays. The effects of droplet collisions and aerodynamic breakups are included in the computations. Octane was the fuel originally used in the combustion. Properties of several other hydrocarbon fuels are provided in the subroutine fuel, so that the combustion of other fuels can be simulated. However, Jet-A properties are not included. Detailed descriptions of the equations and the numerical method of solution are discussed in reference 4.

## MODIFICATION OF KIVA-II

### Jet-A Fuel Properties

In order to use Jet-A as the fuel for combustion, the properties of Jet-A were implemented in the subroutine fuel. The information includes the following.

Chemical symbol,  $C_{12}H_{23}$   
Molecular weight, 176.315  
Critical temperature, 668 K  
Heat of formation (0 K), 72.53 Kcal/mole  
Surface tension (350 K), 18.85 dynes/cm

The enthalpies, latent heat, vapor pressure, and liquid viscosities of Jet-A fuel are given in appendix A from a computer printout.

### Modification of Subroutine "RINPUT"

Because the number of species appearing in the combustion of propane is different from that of the combustion of octane, the enthalpy data of species must be modified in the subroutine RINPUT. The numbers of species for 131, 45, and 5 chemical reactions are 40, 27, and 12, respectively. The enthalpy data in the subroutine RINPUT are arranged according to the order of species appearing in the reactions. All the data are listed in the temperature range from 0 to 5000 K in increments of 100 K. A list of the 40 species is given below.

$C_3H_8$ ,  $O_2$ ,  $N_2$ ,  $CO_2$ ,  $H_2O$ ,  $H$ ,  $H_2$ ,  $O$ ,  $N$   
 $OH$ ,  $CO$ ,  $NO$ ,  $CH$ ,  $CH_2$ ,  $CH_3$ ,  $CH_2O$ ,  $CH_3O$   
 $C_2H_3$ ,  $C_2H_5$ ,  $C_2H_6$ ,  $C_3H_7$ ,  $HCO$ ,  $HO_2$ ,  $NO_2$ ,  $CH_4$ ,  $C_2H_2$   
 $C_2H_4$ ,  $CN$ ,  $C_2H$ ,  $C_2HO$ ,  $HCN$ ,  $HNCO$ ,  $HNO$ ,  $HNO_2$   
 $HNO_3$ ,  $H_2O_2$ ,  $NCO$ ,  $NH$ ,  $NH_2$ ,  $N_2O$

A list of enthalpies for the 40 species appears in appendix B.

### Modification of Input Data File

The major change is in the data provided for the chemical kinetics. As an example, the input file for the simplified chemical mechanism is shown in appendix C.

### JUSTIFICATION OF THREE MECHANISMS FOR THE COMBUSTION OF PROPANE WITH AIR

The full mechanism, consisting of 131 chemical reactions, is considered to be the standard for this evaluation. This standard is established through two extensive studies. In the first study (ref. 1) the numerical predictions of pollutants NO and CO were compared with experimental measurements. They were found to be in good agreement. In the second study (ref. 2) the number of reaction equations was already 131. The full mechanism was further supported by the ignition delay time checked with the shock tube data.

The mechanism with 45 reactions has been considered to be the first possible reduced mechanism for saving computer memory capacity and CPU time. The 45 reactions were determined through sensitivity analysis by mixing propane and air in a container with a definite volume. The results of temperature, pressure, and species concentrations versus time from 45 reactions were compared with those from the full mechanism. They were in fairly good agreement (ref. 2).

The combustion of propane in the simplified mechanism consists of five reactions. Two of the equations are obtained from Westbrook and Dryer (ref. 3), and the other three are from the original input file of KIVA-II describing the extended  $\text{NO}_x$  Zeldovich mechanism. In addition, the six equilibrium reactions described in reference 5 are also used with this five-kinetics-reaction mechanism. The five reactions, together with the reaction constants, are given below.

1.  $\text{C}_3\text{H}_8 + (3/2 + 8/4) \text{O}_2 = 3\text{CO} + 4 \text{H}_2\text{O}$   
 $k_f = 10^{12} \text{Exp}(-30/RT) [\text{C}_3\text{H}_8]^{0.1} [\text{O}_2]^{1.65}$   
 $K_b = 0$
2.  $\text{CO} + 1/2 \text{O}_2 = \text{CO}_2$   
 $K_f = 10^{14.6} \text{Exp}(-40/RT) [\text{CO}]^1 [\text{H}_2\text{O}]^{0.5} [\text{O}_2]^{0.25}$   
 $K_b = 5 \times 10^8 \text{Exp}(-40/RT) [\text{CO}_2]^1$
3.  $\text{O}_2 + 2\text{N}_2 = 2\text{N} + 2\text{NO}$   
 $K_f = 1.5587 \times 10^{14} \text{Exp}(-6.7627 \times 10^4/T) [\text{O}_2] [\text{N}_2]^2$   
 $K_b = 7.500 \times 10^{12} \text{Exp}(0) [\text{N}]^2 [\text{NO}]^2$
4.  $2\text{O}_2 + \text{N}_2 = 2\text{O} + 2\text{NO}$   
 $K_f = 2.6484 \times 10^{10} \text{Exp}(-5.9418 \times 10^4/T) [\text{O}_2]^2 [\text{N}_2]$   
 $K_b = 1.6 \times 10^9 \text{Exp}(-1.9678 \times 10^4/T) [\text{O}]^2 [\text{NO}]^2$
5.  $\text{N}_2 + 2\text{OH} = 2\text{H} + 2\text{NO}$   
 $K_f = 2.123 \times 10^{14} \text{Exp}(-5.7020 \times 10^4/T) [\text{N}]^2 [\text{OH}]^2$   
 $K_b = 0$

## RESULTS AND DISCUSSION

### Comparisons With Data of Direct-Injection Stratified-Charge

#### Piston Engine Combustion

The three mechanisms of propane chemical kinetics were tested first in KIVA-II with computations of direct-injection stratified-charge (DISC) combustion in gasoline-fueled piston engines. The specifications and test conditions for the piston-cylinder configuration are listed in table I. For these calculations, the numerical grid consists of 20 grid points in the axial direction and 22 grid points in the radial direction. A Bessel function velocity profile (ref. 4) was used to simulate the swirl velocity profile of the incoming air. Standard boundary conditions were used in this two-dimensional axisymmetric engine model and the details are described in reference 4.

The three mechanisms of propane chemical kinetics were evaluated by comparisons of data obtained from the numerical simulations of the DISC piston engine. In all test cases, the simulations were started at the beginning of the compression stroke and ended at the crankangle of 65° ATDC. For the baseline case, case 1, a quasi-global mechanism of isooctane oxidation was used together with the extended NO<sub>x</sub> Zeldovich mechanism and six equilibrium reactions (ref. 5). The propane chemical kinetics mechanism for case 2 consists of five kinetic reactions and six equilibrium reactions (these six equilibrium reactions are the same reactions considered in case 1). In addition, the 45-reaction mechanism and the 131-reaction mechanism of propane oxidation were also examined (cases 3 and 4). Table I summarizes the test conditions for cases 1 and 2. For cases 3 and 4, the starting crankangle of ignition was set at 27° BTDC for an ignition duration of 9.6 degrees. In all cases studied, liquid isooctane was injected starting from 52° BTDC for an injection duration of 12.672 degrees in an amount that corresponded to an overall equivalence ratio of about 1.0.

Figures 1 and 2 show the computed mean gas velocity, fuel spray, temperature profile, fuel vapor, and CO profiles at a crankangle of about 29° and 13° BTDC for cases 1 and 2. Comparisons of these results indicate that the five-reaction mechanism of propane oxidation (case 2) predicts a similar combustion rate and slightly lower maximum flame temperature compared with the results predicted by the four-reaction mechanism of isooctane oxidation (case 1). These results also indicate that the flame temperatures are lower than the corresponding local equilibrium temperature.

Figures 3 and 4 show the computed mean gas velocity, fuel spray, temperature, and fuel vapor profile near TDC for cases 3 and 4. It may be seen that the flame is not well propagated and diffusive throughout the engine chamber. The temperature plots of figures 3 and 4 reveal that the predicted maximum flame temperature concentrates only within a small region downstream of the injector tip. This observed low combustion efficiency is probably due to poor fuel-air mixing, ignition, and combustion rate as a result of non-optimal engine design and test conditions. The maximum flame temperatures observed for cases 3 and 4 are lower than the corresponding equilibrium values. The observed flame temperature from the mechanism of 45 reactions is lower than that of the full mechanism. This indicates that in the 45-reaction mechanism

more endothermic reactions and fewer exothermic reactions are considered on a relative basis.

### Comparisons With Data of Model Airblast Fuel Nozzle/Reactive Flow

The model airblast-type fuel nozzle used in this study is shown in figure 4. It is a typical fuel nozzle used in gas turbine combustors. It embodies inner and outer airstreams which help to atomize and distribute fuel sheared from a thin annular sheet. The model fuel nozzle injected fuel by means of an annular fuel passage with the nozzle tip exit area of  $0.03 \text{ cm}^2$ . The fuel exit area is defined by the tip of the core inner air pipe and the position of the wedge-shaped fuel-filming lip of the fuel flow passage. No swirl is imparted to the fuel flow. This fuel nozzle produces a hollow-cone fuel spray with a nominal included angle of 75 degrees. The nonswirl inner air is supplied to the core air pipe with exit an diameter of 1.0 cm. The outer airflow is swirled by a vane assembly. Different vane assembly designs were evaluated. The end cap of the outer air shroud imparts a radial-inflow component to this airflow; the end cap exit area is  $3.24 \text{ cm}^2$ .

The flowfield downstream of the fuel nozzle is axisymmetric without confinement. For these calculations, the numerical grid consists of 60 grid points in the axial direction and 52 grid points in the radial direction. Boundary conditions are applied to the inlet, outlet, solid walls of the fuel nozzle, and centerline of the unconfined flow downstream of the fuel nozzle. A brief description of these boundary conditions are as follows. In this work, the effect of outer air swirler designs on fuel atomization and spray patterns is examined. For the baseline case, the outer air inlet flow is assumed to have a zero mean radial velocity and is characterized by a uniform axial velocity and pressure and an azimuthal velocity profile of a solid body rotation. The inner air is assumed to have zero mean radial and azimuthal velocity, and enters the core air pipe with uniform axial velocity and pressure. The temperature of the inner and outer air is assumed uniform and equal to 1367 K. The profiles of turbulent kinetic energy and turbulent length scale are taken from reference 6. At the solid walls the velocity component normal to the wall is set to zero while the law of the wall is applied to the velocity component parallel to the wall. The normal gradient of turbulent kinetic energy near the wall is set to zero and the dissipation rate of turbulent energy is calculated by using an equilibrium boundary layer. The turbulent length scale is assumed to vary linearly with distance from the solid walls. At the unconfined flow centerline both the radial and azimuthal velocity components are zero, while the radial derivatives of the other flow quantities are zero for reasons of symmetry. The model airblast fuel nozzle is sized for nominal inner air, outer air, and fuel flow rates of 1.3 gm/sec, respectively. A Rosin-Rammler droplet distribution function is used. The calculations are performed with a time step corresponding to  $5 \times 10^{-6}$  sec, and  $3 \times 10^5$  droplet parcels are injected at each time step.

### CONCLUSIONS

Throughout this work it can be seen that the numerical simulation of octane combustion in KIVA-II is used as a guide for propane combustion because accurate experimental data for octane combustion are well known and available

for direct comparison for cascade validation. On the other hand, the adiabatic flame temperature of propane combustion is another checkpoint to be considered. When the air temperature is 1033 K, the propane temperature 311 K and the pressure 1 atm, the adiabatic flame temperature is 2560 K. Because of the vaporization of liquid fuel, either Jet-A or octane, and the heat transfer to the surroundings, the flame temperature is lower than the adiabatic flame temperature.

All simulations are carried out on the CRAY X-MP computer at the NASA Lewis Research Center. Because the chemical kinetics are only a part of the whole simulation, the changes in the CPU time and memory space which can be directly attributed to the kinetic mechanisms for three different mechanisms cannot be clearly accounted for at the present time. Consequently, no definite numbers are reported.

In the prediction of pollutants  $\text{NO}_x$  and CO, it is observed that the full mechanism of 131 reactions is more reliable than the other two mechanisms.

Under the same conditions stated above, a comparison between the combustion of octane and propane is made. The profiles of velocity and temperature are presented in figures 5(a) and (b). These simulations are performed with the understanding that, for the first 1000 cycles of calculations, the combustor is filled only with the airflow, the fuels are injected after 1000 cycles and then ignited. The ignitor is located on the fuel path. The amount of fuel is nearly stoichiometric. The chemical kinetics for the combustion of octane consist of 4 reactions, and for propane 5 reactions. The mechanisms of 131 and 45 reactions are to be investigated in the near future.

#### ACKNOWLEDGMENTS

This project was carried out under NASA Research Grant No. NAG 31112. The information and comments from Ms. B. McBride and Dr. D. Bittker are appreciated.

# APPENDIX A

## JET-A FUEL PROPERTIES

```

-
c +++
c +++ THE ENTHALPY DATA BELOW ARE COMBINED FROM JET-A(L)
c +++ JET-A (C12H23) IN THE TEMPERATURE OF 0--500K AND JET-A(G) IN THE
c +++ TEMPERATURE OF 600--5000K
      data (hkja(n),n=1,51) / 0.00, 7.562,15.342,22.692,32.082,43.272,
1 54.21, 66.38, 79.61, 93.77,108.71,124.30,140.44,157.08,174.15,
2 191.61,209.42,227.53,245.90,264.51,283.31,302.29,321.42,340.68,
3 360.06,379.52,399.07,418.69,438.37,458.11,477.89,497.72,517.59,
4 537.50,557.44,577.42,597.44,617.49,637.58,657.70,677.85,698.05,
5 710.27,738.52,758.80,779.10,799.41,819.73,840.04,860.34,880.62/
c +++ -----
c +++ the liquid latent heats, in ergs/gm, at intervals t=100(n-1):
c +++ values between 300k and upper limit taken from n.b. vargaftik
c +++ "tables on the thermophysical properties of liquids and gases"
c +++ values are linearly extrapolated back to t=0 k.
c +++ -----
c +++
c +++ Jet-A latent heat values in range 0-500k:
c +++
      data (hlatja(n),n=1,51) /3.792e9,3.598e9,3.405e9,3.208e9,
1 2.842e9,2.425e9,45*0.0/
c +++ -----
c +++ the liquid vapor pressures, in dynes/sq. cm., at intervals
c +++ t=10(n-1). also taken from vargaftik. note that each table
c +++ must contain values beyond tcrit of the fuel to protect against
c +++ over-reaching in subroutine evap. also note that pvap is
c +++ dimensioned at lvap words in common /lek/ in comdeck comd;
c +++ lvap must be adequate for all fuels in the library.
c +++ for heptane, dodecane, tridecane and
c +++ hexadecane, the vapor pressure is scaled with temperature
c +++ using eqn (see reid, prop. of liq. and gas. eqn 6-2.4,2.5)
c +++  $\ln(pv)-\ln(pv0)=(\ln(pv1)-\ln(pv0))*((t-t0)/(t1-t0))*t1/t$ 
c +++ w/ t1=tcrit, t0=520k (dodecane), t0=510k (tridecane)
c +++ -----
c +++
c +++ Jet-A vapor pressure every 10k in range 10-690k (tcrit=668k):
c +++
      data (pvapja(n),n=1,69) /.00E+00,.00E+00,.00E+00,.00E+00,.00E+00,
1 .00E+00,.00E+00,.00E+00,.00E+00,.29E-09,.18E-07,.57E-06,.11E-04,
2 .13E-03,.11E-02,.76E-02,.41E-01,.18E+00,.68E+00,.23E+01,.67E+01,
3 .18E+02,.44E+02,.10E+03,.22E+03,.44E+03,.84E+03,.15E+04,.27E+04,
4 .45E+04,.74E+04,.12E+05,.18E+05,.27E+05,.40E+05,.57E+05,.80E+05,
5 .11E+06,.15E+06,.20E+06,.27E+06,.35E+06,.45E+06,.57E+06,.72E+06,
6 .90E+06,.11E+07,.14E+07,.16E+07,.20E+07,.24E+07,.28E+07,.33E+07,
7 .39E+07,.45E+07,.53E+07,.61E+07,.70E+07,.80E+07,.91E+07,.10E+08,
8 .12E+08,.13E+08,.15E+08,.16E+08,.18E+08,.20E+08,.22E+08,.24E+08/
c +++ -----
c +++ the liquid viscosities, in gm/(cm sec). as in the vapor pressures
c +++ above, the intervals are t=10(n-1), and the tables contain values
c +++ beyond tcrit of the fuel. note the visual extrapolation required
c +++ for dodecane, tridecane, tetradecane and hexadecane, for lack of
c +++ tabular data. this needs improvement, esp. around tcrit.
c +++
c +++ Jet-A liquid viscosity every 10k from 0-410k (tcrit=668k) data
c +++ obtained from HB of Aviation Fuel Properties 1984.
c +++
      data (vislqja(n),n=1,42) /23*0.1482,0.08811,0.05607,0.03845,
1 0.02804,0.02163,0.01722,0.01386,0.01161,0.00985,0.00857,0.00745,
2 0.00657,0.00573,0.00529,0.00473,0.00433,0.00392,0.00360,0.00336/
c
c
c

```

# APPENDIX B ENTHALPIES OF ADDITIONAL SPECIES

```

C ***
C *** CH
C ***
data (hk(n,13),n=1,51)/-2.061,-1.342,-0.485, 0.013, 0.711, 1.411,
1 2.12, 2.83, 3.54, 4.31, 5.07, 5.85, 6.65, 7.47, 8.30,
2 9.15, 10.02, 10.90, 11.79, 12.69, 13.60, 14.53, 15.46, 16.41,
3 17.36, 18.32, 19.28, 20.26, 21.23, 22.22, 23.21, 24.20, 25.20,
4 26.20, 27.21, 28.22, 29.23, 30.25, 31.26, 32.23, 33.30, 34.32,
5 35.34, 36.37, 37.39, 38.41, 39.44, 40.46, 41.48, 42.50, 43.52/

C ***
C *** CM2
C ***
data (hk(n,14),n=1,51)/-2.375,-1.581,-0.785, 0.015, 0.833, 1.679,
1 2.56, 3.47, 4.43, 5.41, 6.44, 7.50, 8.60, 9.73, 10.88,
2 12.06, 13.26, 14.48, 15.72, 16.98, 18.25, 19.56, 20.83, 22.14,
3 23.46, 24.79, 26.13, 27.47, 28.82, 30.17, 31.53, 32.89, 34.26,
4 35.63, 37.00, 38.38, 39.76, 41.14, 42.52, 43.91, 45.29, 46.68,
5 48.07, 49.47, 50.86, 52.26, 53.66, 55.06, 56.46, 57.87, 59.28/

C ***
C *** CH3
C ***
data (hk(n,15),n=1,51)/-2.477,-1.682,-0.845, 0.017, 0.975, 2.012,
1 3.12, 4.31, 5.56, 6.88, 8.25, 9.69, 11.17, 12.70, 14.26,
2 15.87, 17.51, 19.18, 20.88, 22.60, 24.34, 26.11, 27.89, 29.69,
3 31.51, 33.33, 35.17, 37.02, 38.88, 40.76, 42.61, 44.49, 46.37,
4 48.26, 50.15, 52.05, 53.95, 55.85, 57.74, 59.67, 61.58, 63.50,
5 65.42, 67.34, 69.27, 71.20, 73.13, 75.06, 77.00, 78.94, 80.89/

C ***
C *** CH20
C ***
data (hk(n,16),n=1,51)/-2.375,-1.600,-0.803, 0.016, 0.905, 1.894,
1 2.99, 4.20, 5.49, 6.87, 8.31, 9.82, 11.38, 12.98, 14.62,
2 16.29, 18.00, 19.74, 21.50, 23.29, 25.09, 26.91, 28.75, 30.60,
3 32.46, 34.34, 36.22, 38.11, 40.00, 41.90, 43.80, 45.71, 47.62,
4 49.54, 51.45, 53.37, 55.29, 57.22, 59.14, 61.07, 63.00, 64.93,
5 66.87, 68.81, 70.75, 72.69, 74.64, 76.58, 78.54, 80.49, 82.45/

C ***
C *** CH30
C ***
data (hk(n,17),n=1,51)/-2.431,-1.636,-0.836, 0.017, 1.003, 2.157,
1 3.48, 4.76, 6.07, 7.42, 8.83, 10.29, 11.77, 13.26, 14.76,
2 16.20, 18.00, 19.74, 21.50, 23.29, 25.09, 26.91, 28.75, 30.60,
3 32.46, 34.34, 36.22, 38.11, 40.00, 41.90, 43.80, 45.71, 47.62,
4 49.54, 51.45, 53.37, 55.29, 57.22, 59.14, 61.07, 63.00, 64.93,
5 66.87, 68.81, 70.75, 72.69, 74.64, 76.58, 78.54, 80.49, 82.45/

C ***
C *** CH23
C ***
data (hk(n,18),n=1,51)/-2.458,-1.643,-0.860, 0.018, 1.046, 2.246,
1 3.61, 4.92, 6.26, 7.63, 9.04, 10.49, 11.97, 13.46, 14.96,
2 16.47, 18.30, 20.14, 21.99, 23.85, 25.72, 27.60, 29.49, 31.38,
3 33.28, 35.18, 37.09, 39.00, 40.92, 42.84, 44.76, 46.68, 48.60,
4 50.51, 52.43, 54.35, 56.27, 58.19, 60.11, 62.03, 63.95, 65.87,
5 67.79, 69.71, 71.63, 73.55, 75.47, 77.39, 79.31, 81.23, 83.15/

C ***
C *** CH25
C ***
data (hk(n,19),n=1,51)/-2.939,-2.100,-1.101, 0.023, 1.394, 3.015,
1 4.87, 6.93, 9.17, 11.55, 14.08, 16.72, 19.47, 22.31, 25.23,
2 28.22, 31.24, 34.40, 37.58, 40.80, 44.06, 47.36, 50.67, 54.05,
3 57.43, 60.84, 64.26, 67.70, 71.16, 74.62, 78.10, 81.58, 85.07,
4 88.57, 92.08, 95.59, 99.11, 102.63, 106.16, 109.68, 113.21, 116.77,
5 120.32, 123.88, 127.44, 131.01, 134.59, 138.17, 141.74, 145.36, 148.96/

C ***
C *** CH26
C ***
data (hk(n,20),n=1,51)/-2.842,-2.033,-1.104, 0.023, 1.430, 3.138,
1 5.16, 7.40, 9.88, 12.55, 15.39, 18.39, 21.51, 24.73, 28.08,
2 31.51, 35.02, 38.61, 42.24, 45.92, 49.73, 53.54, 57.39, 61.27,
3 65.19, 69.14, 73.10, 77.09, 81.10, 85.12, 89.16, 93.20, 97.26,
4 101.33, 105.40, 109.48, 113.57, 117.66, 121.77, 125.87, 129.99, 134.11,
5 138.24, 142.37, 146.51, 150.66, 154.82, 158.99, 163.16, 167.34, 171.52/

C ***
C *** CH27
C ***
data (hk(n,21),n=1,51)/-3.373,-2.487,-1.403, 0.030, 1.498, 4.200,
1 6.70, 9.95, 13.28, 16.84, 20.61, 24.58, 28.69, 32.93, 37.30,
2 41.77, 46.33, 50.98, 55.71, 60.50, 65.35, 70.26, 75.21, 80.19,
3 85.21, 90.26, 95.34, 100.45, 105.56, 110.67, 115.81, 120.96, 126.11,
4 131.28, 136.45, 141.63, 146.82, 152.01, 157.21, 162.41, 167.62, 172.84,
5 178.06, 183.29, 188.53, 193.77, 199.03, 204.29, 209.56, 214.84, 220.13/

C ***
C *** HCO
C ***
data (hk(n,22),n=1,51)/-2.587,-1.593,-0.796, 0.015, 0.864, 1.760,
1 2.71, 3.71, 4.76, 5.85, 6.98, 8.14, 9.32, 10.53, 11.75,
2 12.99, 14.25, 15.53, 16.82, 18.11, 19.42, 20.74, 22.07, 23.40,
3 24.74, 26.09, 27.44, 28.79, 30.15, 31.51, 32.88, 34.25, 35.62,
4 36.99, 38.34, 39.74, 41.12, 42.50, 43.89, 45.27, 46.66, 48.05,
5 49.44, 50.84, 52.24, 53.64, 55.04, 56.44, 57.85, 59.26, 60.67/

C ***
C *** H2O
C ***
data (hk(n,23),n=1,51)/-2.392,-1.598,-0.800, 0.015, 0.878, 1.798,
1 2.77, 3.80, 4.84, 5.94, 7.09, 8.24, 9.42, 10.62, 11.85,
2 13.09, 14.36, 15.64, 16.93, 18.27, 19.60, 20.95, 22.31, 23.67,
3 25.08, 26.44, 27.89, 29.31, 30.74, 32.18, 33.63, 35.09, 36.56,
4 38.01, 39.48, 40.95, 42.43, 43.92, 45.40, 46.89, 48.39, 49.88,
5 51.37, 52.87, 54.37, 55.87, 57.37, 58.86, 60.36, 61.86, 63.36/

C ***
C *** H2O2
C ***
data (hk(n,24),n=1,51)/-2.440,-1.645,-0.839, 0.016, 0.944, 1.949,
1 3.03, 4.16, 5.35, 6.57, 7.82, 9.10, 10.39, 11.70, 13.02,
2 14.34, 15.71, 17.07, 18.44, 19.82, 21.21, 22.60, 24.01, 25.42,
3 26.84, 28.26, 29.70, 31.13, 32.58, 34.05, 35.49, 36.95, 38.42,
4 39.90, 41.38, 42.87, 44.37, 45.87, 47.39, 48.91, 50.43, 51.97,
5 53.52, 55.07, 56.63, 58.20, 59.79, 61.38, 62.97, 64.58, 66.20/

C ***
C *** CH4
C ***
data (hk(n,25),n=1,51)/-2.396,-1.603,-0.805, 0.016, 0.924, 1.962,
1 3.15, 4.48, 5.95, 7.53, 9.24, 11.04, 12.94, 14.91, 16.96,
2 18.08, 20.26, 22.50, 24.80, 27.14, 29.52, 31.94, 34.40, 36.90,
3 39.42, 42.08, 44.84, 47.68, 50.58, 53.50, 56.44, 59.40, 62.38,
4 64.17, 66.92, 69.67, 72.43, 75.20, 77.99, 80.80, 83.62, 86.45,
5 89.30, 92.16, 95.04, 97.94, 100.84, 103.77, 106.71, 109.66, 112.63/

C ***
C *** C2H2
C ***
data (hk(n,26),n=1,51)/-2.371,-1.696,-0.938, 0.019, 1.151, 2.407,
1 3.75, 5.18, 6.66, 8.20, 9.79, 11.44, 13.12, 14.85, 16.61,
2 18.40, 20.23, 22.08, 23.94, 25.85, 27.77, 29.71, 31.66, 33.63,
3 35.42, 37.61, 39.82, 41.84, 43.86, 45.70, 47.74, 49.79, 51.85,
4 53.92, 55.99, 58.07, 60.16, 62.25, 64.35, 66.46, 68.57, 70.69,
5 72.82, 74.95, 77.09, 79.23, 81.38, 83.54, 85.70, 87.87, 90.05/

C ***
C *** C2H4
C ***

```

```

C ***
C *** data (hk(n,27),n=1,51)/-2.514,-1.719,-0.909, 0.019, 1.141, 2.535,
1 4.13, 5.71, 7.35, 9.02, 10.70, 12.40, 14.10, 15.80, 17.50,
2 19.20, 20.99, 22.79, 24.59, 26.38, 28.18, 29.98, 31.78, 33.58,
3 35.38, 37.18, 38.98, 40.78, 42.58, 44.38, 46.18, 47.98, 49.78,
4 51.58, 53.38, 55.18, 56.98, 58.78, 60.58, 62.38, 64.18, 65.98,
5 67.78, 69.58, 71.38, 73.18, 74.98, 76.78, 78.58, 80.38, 82.18/

C ***
C *** CH
C ***
data (hk(n,28),n=1,51)/-2.073,-1.390,-0.683, 0.013, 0.713, 1.422,
1 2.15, 2.87, 3.65, 4.42, 5.22, 6.02, 6.83, 7.64, 8.49,
2 9.35, 10.19, 11.05, 11.93, 12.81, 13.71, 14.62, 15.54, 16.47,
3 17.41, 18.36, 19.32, 20.29, 21.27, 22.26, 23.26, 24.27, 25.29,
4 26.31, 27.35, 28.39, 29.43, 30.47, 31.55, 32.62, 33.69, 34.77,
5 35.85, 36.93, 38.02, 39.12, 40.21, 41.31, 42.41, 43.52, 44.62/

C ***
C *** C2H
C ***
data (hk(n,29),n=1,51)/-2.356,-1.600,-0.886, 0.018, 1.002, 2.041,
1 3.12, 4.24, 5.40, 6.60, 7.84, 9.12, 10.45, 11.81, 13.20,
2 14.62, 16.04, 17.53, 19.01, 20.52, 22.02, 23.56, 25.10, 26.65,
3 28.20, 29.76, 31.32, 32.88, 34.45, 36.01, 37.58, 39.14, 40.70,
4 42.24, 43.82, 45.38, 46.93, 48.48, 50.03, 51.58, 53.12, 54.67,
5 56.21, 57.74, 59.28, 60.82, 62.35, 63.89, 65.42, 66.95, 68.48/

C ***
C *** CHCO
C ***
data (hk(n,30),n=1,51)/-2.636,-1.888,-1.004, 0.020, 1.149, 2.359,
1 3.63, 4.97, 6.36, 7.81, 9.31, 10.84, 12.44, 14.07, 15.72,
2 17.41, 19.12, 20.86, 22.62, 24.40, 26.20, 28.02, 29.85, 31.69,
3 33.54, 35.41, 37.28, 39.16, 41.06, 42.94, 44.85, 46.74, 48.64,
4 50.55, 52.47, 54.38, 56.30, 58.23, 60.15, 62.08, 64.01, 65.94,
5 67.87, 69.81, 71.75, 73.69, 75.64, 77.58, 79.53, 81.48, 83.44/

C ***
C *** HCHO
C ***
data (hk(n,31),n=1,51)/-2.207,-1.513,-0.794, 0.016, 0.915, 1.883,
1 2.91, 3.98, 5.09, 6.24, 7.42, 8.64, 9.88, 11.14, 12.43,
2 13.74, 15.07, 16.42, 17.78, 19.15, 20.54, 21.96, 23.35, 24.77,
3 26.20, 27.57, 28.97, 30.37, 31.77, 33.17, 34.58, 35.98, 37.38,
4 39.80, 41.17, 42.55, 43.93, 45.32, 46.70, 48.19, 49.68, 51.17,
5 52.67, 54.16, 55.64, 57.16, 58.66, 60.17, 61.67, 63.18, 64.69/

C ***
C *** H2CO
C ***
data (hk(n,32),n=1,51)/-2.620,-1.826,-0.980, 0.020, 1.167, 2.432,
1 3.79, 5.22, 6.71, 8.26, 9.85, 11.48, 13.15, 14.84, 16.56,
2 18.31, 20.08, 21.87, 23.68, 25.50, 27.34, 29.17, 31.06, 32.93,
3 34.81, 36.70, 38.60, 40.50, 42.41, 44.32, 46.23, 48.15, 50.08,
4 52.00, 53.93, 55.86, 57.79, 59.73, 61.66, 63.60, 65.56, 67.49,
5 69.45, 71.38, 73.33, 75.28, 77.23, 79.18, 81.14, 83.10, 85.06/

C ***
C *** H2O
C ***
data (hk(n,33),n=1,51)/-2.376,-1.582,-0.786, 0.015, 0.842, 1.715,
1 2.64, 3.62, 4.65, 5.75, 6.85, 8.02, 9.22, 10.46, 11.73,
2 13.05, 14.37, 15.73, 17.12, 18.54, 19.97, 21.43, 22.91, 24.40,
3 25.91, 27.45, 28.97, 30.51, 32.07, 33.63, 35.21, 36.78, 38.37,
4 39.96, 41.55, 43.14, 44.73, 46.33, 47.93, 49.52, 51.11, 52.71,
5 54.30, 55.89, 57.47, 59.05, 60.63, 62.21, 63.78, 65.35, 66.92/

C ***
C *** H2O2
C ***
data (hk(n,34),n=1,51)/-2.772,-1.928,-1.016, 0.021, 1.197, 2.476,
1 3.90, 5.28, 6.72, 8.21, 9.75, 11.32, 12.92, 14.55, 16.21,
2 18.79, 20.58, 22.40, 24.23, 26.07, 27.93, 29.80, 31.68, 33.58,
3 35.47, 37.37, 39.28, 41.19, 43.11, 45.03, 46.94, 48.89, 50.82,
4 52.75, 54.69, 56.62, 58.56, 60.51, 62.46, 64.41, 66.39, 68.29,
5 70.24, 72.19, 74.14, 76.10, 78.05, 80.01, 81.97, 83.94, 85.90/

C ***
C *** H2O3
C ***
data (hk(n,35),n=1,51)/-2.838,-2.041,-1.159, 0.024, 1.442, 3.071,
1 4.87, 6.80, 8.83, 10.94, 13.10, 15.31, 17.56, 19.83, 22.13,
2 24.45, 26.80, 29.16, 31.53, 33.92, 36.32, 38.74, 41.16, 43.58,
3 46.02, 48.45, 50.90, 53.36, 55.79, 58.23, 60.68, 63.13, 65.59,
4 68.04, 70.49, 72.94, 75.39, 77.85, 80.30, 82.76, 85.21, 87.67,
5 90.13, 92.59, 95.05, 97.52, 99.98, 102.45, 104.92, 107.39, 109.86/

C ***
C *** H2O2
C ***
data (hk(n,36),n=1,51)/-2.667,-1.845,-0.952, 0.019, 1.080, 2.254,
1 3.47, 4.79, 6.16, 7.58, 9.05, 10.56, 12.11, 13.69, 15.31,
2 16.95, 18.62, 20.32, 22.04, 23.77, 25.53, 27.31, 29.10, 30.90,
3 32.72, 34.55, 36.40, 38.25, 40.11, 41.98, 43.84, 45.75, 47.64,
4 49.54, 51.45, 53.36, 55.28, 57.21, 59.16, 61.07, 63.01, 64.94,
5 66.91, 68.86, 70.83, 72.79, 74.74, 76.74, 78.72, 80.70, 82.69/

C ***
C *** HCO
C ***
data (hk(n,37),n=1,51)/-2.443,-1.691,-0.870, 0.018, 1.024, 2.111,
1 3.24, 4.47, 5.73, 7.02, 8.34, 9.69, 11.05, 12.42, 13.81,
2 15.21, 16.63, 18.05, 19.48, 20.92, 22.34, 23.81, 25.26, 26.72,
3 28.18, 29.64, 31.11, 32.57, 34.06, 35.51, 36.98, 38.45, 39.92,
4 41.40, 42.87, 44.34, 45.81, 47.27, 48.74, 50.26, 51.71, 53.19,
5 54.66, 56.14, 57.62, 59.10, 60.57, 62.06, 63.54, 65.02, 66.50/

C ***
C *** NH
C ***
data (hk(n,38),n=1,51)/-2.056,-1.384,-0.685, 0.013, 0.710, 1.409,
1 2.11, 2.82, 3.54, 4.26, 5.01, 5.76, 6.53, 7.31, 8.10,
2 8.90, 9.71, 10.53, 11.34, 12.20, 13.05, 13.90, 14.74, 15.63,
3 16.51, 17.59, 18.68, 19.78, 20.84, 21.91, 22.83, 23.75,
4 24.69, 25.83, 26.97, 28.11, 29.26, 30.41, 31.56, 32.72,
5 33.34, 34.53, 35.73, 36.93, 38.13, 39.36, 40.58, 41.80/

C ***
C *** H2
C ***
data (hk(n,39),n=1,51)/-2.375,-1.587,-0.788, 0.015, 0.834, 1.679,
1 2.58, 3.47, 4.42, 5.40, 6.43, 7.48, 8.57, 9.69, 10.84,
2 12.01, 13.21, 14.43, 15.67, 16.93, 18.21, 19.51, 20.82, 22.15,
3 23.49, 24.84, 26.21, 27.59, 28.98, 30.38, 31.78, 33.20, 34.63,
4 36.04, 37.50, 38.95, 40.40, 41.87, 43.35, 44.81, 46.27, 47.77,
5 49.27, 50.76, 52.26, 53.77, 55.28, 56.80, 58.32, 59.84, 61.37/

C ***
C *** H2O
C ***
data (hk(n,40),n=1,51)/-2.270,-1.574,-0.850, 0.017, 0.992, 2.052,
1 3.14, 4.37, 5.60, 6.87, 8.18, 9.52, 10.84, 12.23, 13.62,
2 15.02, 16.44, 17.87, 19.31, 20.76, 22.22, 23.68, 25.16, 26.64,
3 28.13, 29.62, 31.11, 32.61, 34.12, 35.63, 37.14, 38.65, 40.16,
4 41.66, 43.20, 44.72, 46.25, 47.78, 49.31, 50.84, 52.38, 53.91,
5 55.45, 56.90, 58.44, 60.09, 61.65, 63.20, 64.76, 66.33, 67.87/

```

ORIGINAL PAGE IS  
OF POOR QUALITY

# APPENDIX C

## INPUT FILE FOR SIMPLIFIED MECHANISM WITH FIVE CHEMICAL REACTIONS

|                                      |         |          |     |
|--------------------------------------|---------|----------|-----|
| T3AAA K011887 13X1X20 2-D COMBUSTOR. | TKESW   | 1.0      |     |
| irest 0                              | sgsl    | 0.0      |     |
| ipost 1                              | uniscal | 0.0      |     |
| nx 13                                | airmul  | 1.457e-5 |     |
| ny 1                                 | airmu2  | 110.0    |     |
| nz 20                                | airla1  | 252.0    |     |
| lwall 1                              | airla2  | 200.0    |     |
| nchop 0                              | expdif  | 0.6      |     |
| lpr 0                                | prl     | 0.74     |     |
| jsectr 1                             | rpr     | 1.11     |     |
| irez 0                               | rprq    | 1.0      |     |
| ncfilm 200                           | rpre    | 0.769231 |     |
| nctap8 9999                          | rsc     | 1.11     |     |
| nclast 4000                          | xignit  | 2.0e+3   |     |
| cafilm 5.0                           | TIIGN   | 0.0      |     |
| cafin 360.0                          | TDIGN   | 9.99E+9  |     |
| cadump -90.0                         | calign  | -27.0    |     |
| dcadmp 10.0                          | cadign  | 9.6      |     |
| angmom 1.0                           | iignl1  | 1        |     |
| cyl 1.0                              | iignr1  | 1        |     |
| dy 0.0                               | jignf1  | 1        |     |
| pgssw 1.0                            | jignd1  | 1        |     |
| sampl 0.0                            | kignb1  | 2        |     |
| dti 1.04167e-4                       | kignt1  | 2        |     |
| dtmxa 9.97e+9                        | iignl2  | 1        |     |
| dtmax 9.99e+9                        | iignr2  | 1        |     |
| tlind 0.0                            | jignf2  | 1        |     |
| twfilm 9.97e+9                       | jignd2  | 1        |     |
| twfin 9.97e+9                        | kignb2  | 2        |     |
| fchsp 0.25                           | kignt2  | 2        |     |
| stroke 0.0                           | kwikey  | 0        |     |
| squish 100.0                         | numnoz  | 1        |     |
| rpm 0.0                              | numvel  | 1        |     |
| atdc 0.0                             | injdist | 1        |     |
| conrod 16.269                        | kolide  | 1        |     |
| offset 0.0                           | tlinj   | 0.0      |     |
| swirl 0.0                            | tdinj   | 9.99e+9  |     |
| swipro 1.01e-10                      | calinj  | -52.0    |     |
| thsect 0.5                           | cadinj  | 12.672   |     |
| epsy 1.0e-3                          | tspmas  | 9.208    |     |
| epsv 1.0e-3                          | pulse   | 0.0      |     |
| epsp 1.0e-4                          | tnparc  | 4000.0   |     |
| epst 1.0e-3                          | rhop    | 0.7436   |     |
| epsk 1.0e-3                          | tpi     | 350.0    |     |
| epse 1.0e-3                          | turb    | 1.0      |     |
| gx 0.0                               | breakup | 1.0      |     |
| gy 0.0                               | evapp   | 1.0      |     |
| gz 0.0                               | drnoz   | 0.0      |     |
| tcylwl 400.0                         | dznoz   | 0.1      |     |
| thead 400.0                          | dthnoz  | 0.0      |     |
| tpistn 400.0                         | tiltxy  | 0.0      |     |
| tvalve 400.0                         | tiltxz  | 0.0      |     |
| TEMPI 400.0                          | cone    | 62.5     |     |
| pardon 0.0                           | dcone   | 12.5     |     |
| a0 0.1                               | anoz    | 1.0      |     |
| b0 1.0                               | smr     | 5.00e-4  |     |
| anc4 0.05                            | amp0    | 0.0      |     |
| adia 0.0                             |         | 4000.0   |     |
| anu0 0.0                             | npo     | 14       |     |
| visrat-.66666667                     | nunif   | 0        |     |
| tcut 800.0                           | 1 1     | 0.0      | 0.0 |
| tcute 1200.0                         | 2 1     | .195     | 0.0 |
| epachm 0.20                          | 3 1     | .391     | 0.0 |
| omgchm 1.0                           | 4 1     | .586     | 0.0 |
| TKEI 2.250E+4                        | 5 1     | .782     | 0.0 |

# APPENDIX C - Continued.

```

6 1 .977 0.0
7 1 1.172 0.0
8 1 1.368 0.0
9 1 1.563 0.0
10 1 1.758 0.0
11 1 1.954 0.0
12 1 2.147 0.0
13 1 2.345 0.0
14 1 2.540 0.0
nho 0
square 0.0
rcornr 0.0
nstrt 0
icont 11101111011110000000011000
mirror 1
nvzone 2
0.0 -5.0 1.0e10 0 0 0 0 0 1 0
-5.0 -45.0 35.0 0 1 1 1 1 1 0
nvvec 4
nvpvec 0
0.0 -45.0 15.0 0 1 0
3.0 -45.0 15.0 0 3 0
0.0 -5.0 1.0e10 0 0 6
0.0 -5.0 1.0e10 0 0 13
nvcont 2
0.0 -45.0 15.0 0 3 0
0.0 -5.0 1.0e10 0 0 6
nsp 12
c3h8 rho1 0.0
a2 rho2 3.1096e-4 mw2 32.000 htf2 0.0
n2 rho3 1.0809e-3 mw3 28.016 htf3 0.0
co2 rho4 1.4007e-5 mw4 44.011 htf4 -93.965
h2o rho5 7.0030e-6 mw5 18.016 htf5 -57.103
h rho6 0.0 mw6 1.008 htf6 51.631
h2 rho7 0.0 mw7 2.016 htf7 0.0
o rho8 0.0 mw8 16.000 htf8 58.989
n rho9 0.0 mw9 14.008 htf9 112.520
oh rho10 0.0 mw10 17.008 htf10 9.289
co rho11 0.0 mw11 28.011 htf11 -27.200
no rho12 0.0 mw12 30.008 htf12 21.456
rtout 0.0
topout 1.0
botin 1.0
distamb 0.0
pamb 1.6229e+6
tkeamb 0.10
sclamb 0.278450
spdamb1 0.0
spdamb2 3.1096e-4
spdamb3 1.0809e-3
spdamb4 1.4007e-5
spdamb5 7.0030e-6
spdamb6 0.0
spdamb7 0.0
spdamb8 0.0
spdamb9 0.0
spdam10 0.0
spdam11 0.0
spdam12 0.0
win 4023.40
spdin01 0.0
spdin02 3.1096e-4
spdin03 1.0809e-3
spdin04 1.4007e-5
spdin05 7.0030e-6

```

```

spdin06 0.0
spdin07 0.0
spdin08 0.0
spdin09 0.0
spdin10 0.0
spdin11 0.0
spdin12 0.0
nrk      5
cf1 1.0000e12 ef1 1.5106e+4 zf1 0.0
cb1 0.0 eb1 0.0 zb1 0.0
am1 2 7 0 0 0 0 0 0 0 0 0 0
bm1 0 0 0 0 8 0 0 0 0 0 6 0
ae1 0.1 1.65 0. 0. 0. 0. 0. 0. 0. 0. 0. 0.
be1 0. 0. 0. 0. 0. 0. 0. 0. 0. 0. 0. 0.
cf2 3.9810e10 ef2 2.0141e+4 zf2 0.0
cb2 5.0000e+0 eb2 2.0141e+4 zb2 0.0
am2 0 1 0 0 0 0 0 0 0 0 2 0
bm2 0 0 0 2 0 0 0 0 0 0 0 0
ae2 0 0.25 0. 0 0.5 0 0 0 0 0 1.0 0
be2 0 0 0 1.0 0 0 0 0 0 0 0 0
cf3 1.5587e14 ef3 6.76276e4 zf3 0.0
cb3 7.5000e12 eb3 0.0000 zb3 0.0
am3 0 1 2 0 0 0 0 0 0 0 0 0
bm3 0 0 0 0 0 0 0 0 2 0 0 2
ae3 0 1.0 2.0 0 0 0 0 0 0 0 0 0
be3 0 0 0 0 0 0 0 0 2.0 0 0 2.0
cf4 2.6484e10 ef4 5.9418e+4 zf4 0.0
cb4 1.6000e+9 eb4 1.9678e+4 zb4 0.0
am4 0 2 1 0 0 0 0 0 0 0 0 0
bm4 0 0 0 0 0 0 0 2 0 0 0 2
ae4 0 2.0 1.0 0 0 0 0 0 0 0 0 0
be4 0 0 1.0 0 0 1.0 0 2.0 0 0 0 2.0
cf5 2.1230e14 ef5 5.70206e4 zf5 0.0
cb5 0.0 eb5 0.0 zb5 0.0
am5 0 0 1 0 0 0 0 0 0 2 0 0
bm5 0 0 0 0 0 2 0 0 0 0 0 2
ae5 0 0 1.0 0 0 0 0 0 0 2.0 0 0
be5 0 0 0 0 0 2.0 0 0 0 0 0 2.0
nre      6
as1 0.990207 bs1 -51.7916 cs1 0.993074 ds1 -0.343428 es1 0.0111668
an1 0 0 0 0 0 0 1 0 0 0 0 0
bn1 0 0 0 0 0 2 0 0 0 0 0 0
as2 0.431310 bs2 -59.6554 cs2 3.503350 ds2 -0.340016 es2 0.0158715
an2 0 1 0 0 0 0 0 0 0 0 0 0
bn2 0 0 0 0 0 0 0 2 0 0 0 0
as3 0.794709 bs3 -113.2080 cs3 3.168370 ds3 -0.443814 es3 0.0269699
an3 0 0 1 0 0 0 0 0 0 0 0 0
bn3 0 0 0 0 0 0 0 0 2 0 0 0
as4 -0.652937 bs4 -7.8232 cs4 3.920330 ds4 0.163490 es4 -0.0142865
an4 0 1 0 0 0 0 1 0 0 0 0 0
bn4 0 0 0 0 0 0 0 0 0 2 0 0
as5 1.158882 bs5 -76.8472 cs5 8.532155 ds5 -0.068320 es5 0.0463471
an5 0 1 0 0 2 0 0 0 0 0 0 0
bn5 0 0 0 0 0 0 0 0 0 4 0 0
as6 0.980875 bs6 68.4453 cs6 -10.5938 ds6 0.574260 es6 -0.0414570
an6 0 1 0 0 0 0 0 0 0 0 2 0
bn6 0 0 0 2 0 0 0 0 0 0 0 0

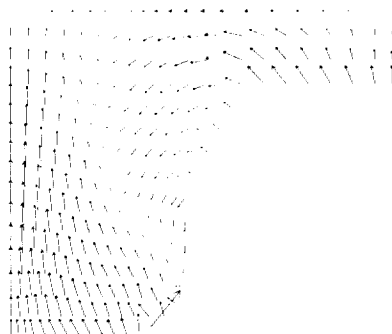
```

## REFERENCES

1. Nguyen, H.L., Bittker, D.A., and Niedzwiecki, R.W., "Investigation of a Low  $\text{NO}_x$  Staged Combustor Concept in High-Speed Civil Transport Engines," AIAA Paper 89-2942, June 1989. (Also, NASA TM-101977).
2. Ying, S.J. and Nguyen, H.L., "Reduced Chemical Kinetics For Propane Combustion," AIAA Paper 90-0546, Jan. 1990.
3. Westbrook, C.K. and Dryer, F.L., "Simplified Reaction Mechanisms for the Oxidation of Hydrocarbon Fuels in Flames," Combustion Science and Technology, Vol. 27, No. 1-2, 1981, pp. 31-43.
4. Amsden, A.A., O'Rourke, P.J., and Butler, T.D., "KIVA-II: A Computer Program For Chemically Reactive Flows With Sprays," Los Alamos National Laboratory Report, LA-11560-MS, May 1989.
5. Amsden, A.A., Ramshaw, J.D., O'Rourke, P.J., Dukowicz, J.K., "KIVA: A Computer Program for Two- and Three-Dimensional Fluid Flows with Chemical Reactions and Fuel Sprays," Los Alamos National Laboratory Report, LA-10245-MS, February 1985.
6. Butler, T. Daniel, "Analysis of an Air Assist Atomizer," Los Alamos National Lab, private communication, May 1990.

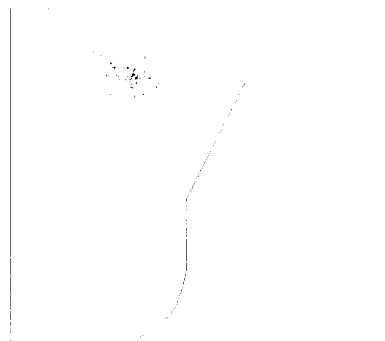
TABLE I. - ENGINE PARAMETERS AND TEST CONDITIONS

|  |           |
|--|-----------|
| Engine stroke, cm                      | 9.55      |
| Compression ratio                      | 6.54      |
| Volume of piston bowl, cm <sup>3</sup> | 58.8      |
| Squish clearance, cm                   | 0.1819    |
| Connecting rod length, cm              | 16.269    |
| rpm                                    | 1600      |
| Initial engine air temperature, K      | 400       |
| Initial engine pressure, atm           | 1         |
| Fuel                                   | isooctane |
| Starting crankangle of injection, deg  | 52 BTDC   |
| Injection duration, deg                | 12.672    |
| Injection angle, deg                   | 60        |
| Starting crankangle of ignition, deg   | 27 BTDC   |
| Ignition duration, deg                 | 9.6       |



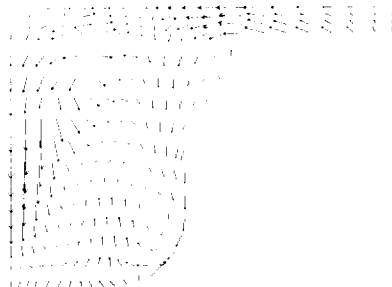
$U_{MAX} = 7.84828E+02$ ,  $V_{MAX} = 2.94169E+03$ ,  
 $W_{MAX} = 9.76695E+02$

(a) GAS VELOCITY AT 29.05° BTDC.



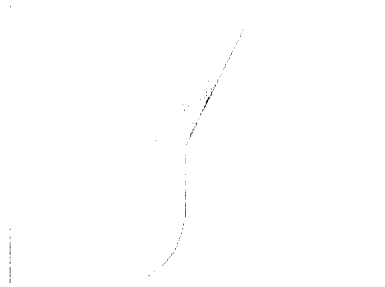
305 PARTICLES IN THE SYSTEM

(b) FUEL SPRAY AT 29.95° BTDC.



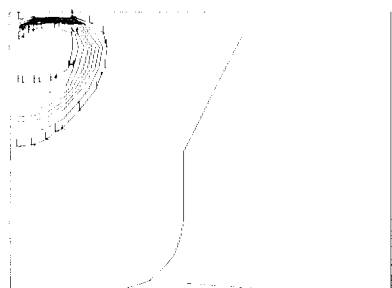
$U_{MAX} = 8.84606E+02$ ,  $V_{MAX} = 3.38367E+03$ ,  
 $W_{MAX} = 1.24565E+03$

(c) GAS VELOCITY AT 11.37° BTDC.



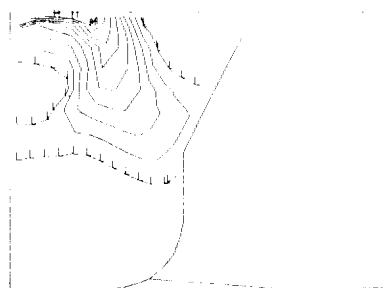
122 PARTICLES IN THE SYSTEM

(d) FUEL SPRAY AT 11.37° BTDC.



$L = 6.57971E+02$ ,  $H = 2.96074E+03$ ,  
 $DQ = 2.30277E+02$

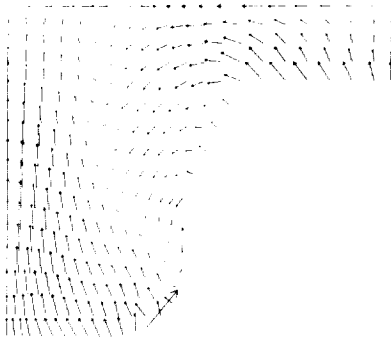
(e) TEMPERATURE AT 11.37° BTDC.



$c_8h_{18}$  ACROSS  $J = 1$  PLANE,  $L = 1.17529E-02$ ,  
 $H = 1.05776E-01$ ,  $11.37^\circ$ ,  $DQ = 1.17529E-02$

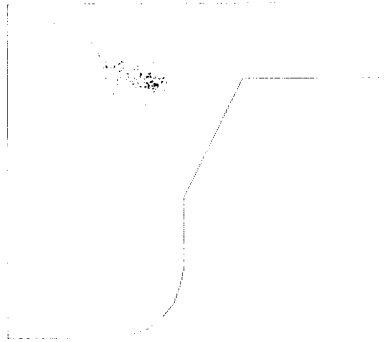
(f) FUEL VAPOR AT 11.37° BTDC.

FIGURE 1. - RESULTS OF DISC GASOLINE-FUELED PISTON ENGINE FOR CASE 1.



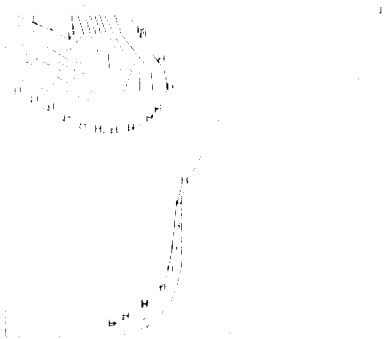
VELOCITY ACROSS J = 1 PLANE,  $-29.17^\circ$ ,  
 $U_{MAX} = 7.86088E+02$ ,  $V_{MAX} = 2.94103E+03$ ,  
 $W_{MAX} = 9.79231E+02$

(a) GAS VELOCITY AT  $29.17^\circ$  BTDC.



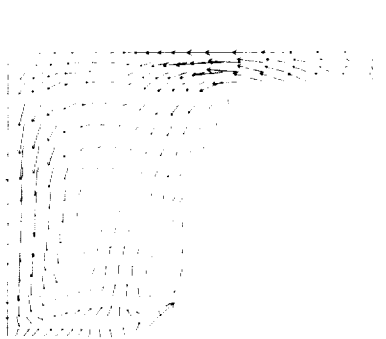
472 PARTICLES IN THE SYSTEM

(b) FUEL SPRAY AT  $29.17^\circ$  BTDC.



$L = 4.83900E+02$ ,  $H = 6.50552E+02$ ,  
 $DQ = 1.66652E+01$

(c) TEMPERATURE AT  $29.17^\circ$  BTDC.



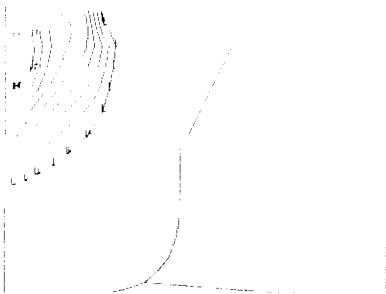
$U_{MAX} = 1.02988E+03$ ,  $V_{MAX} = 3.34960E+03$ ,  
 $W_{MAX} = 1.08345E+03$

(d) GAS VELOCITY AT  $13^\circ$  BTDC.



432 PARTICLES IN THE SYSTEM

(e) FUEL SPRAY AT  $13.89^\circ$  BTDC.



$L = 6.82538E+02$ ,  $H = 2.92452E+03$ ,  
 $DQ = 2.24198E+02$

(f) TEMPERATURE AT  $13.89^\circ$  BTDC.

FIGURE 2. - RESULTS OF DISC GASOLINE-FUELED PISTON ENGINE FOR CASE 2.

ORIGINAL PAGE IS  
 OF POOR QUALITY.

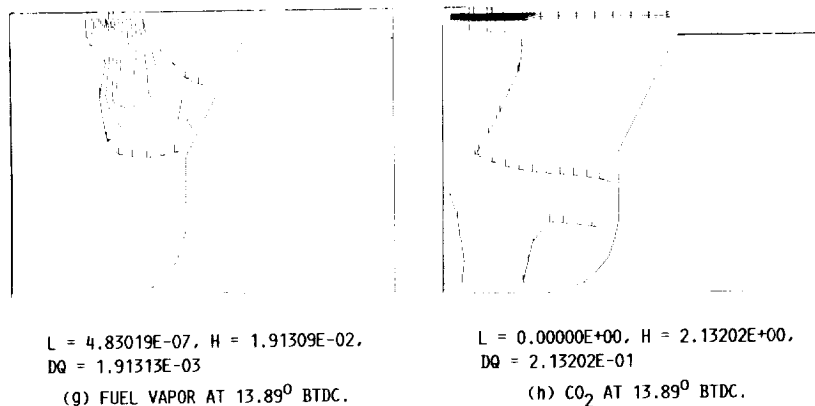


FIGURE 2. - CONCLUDED.

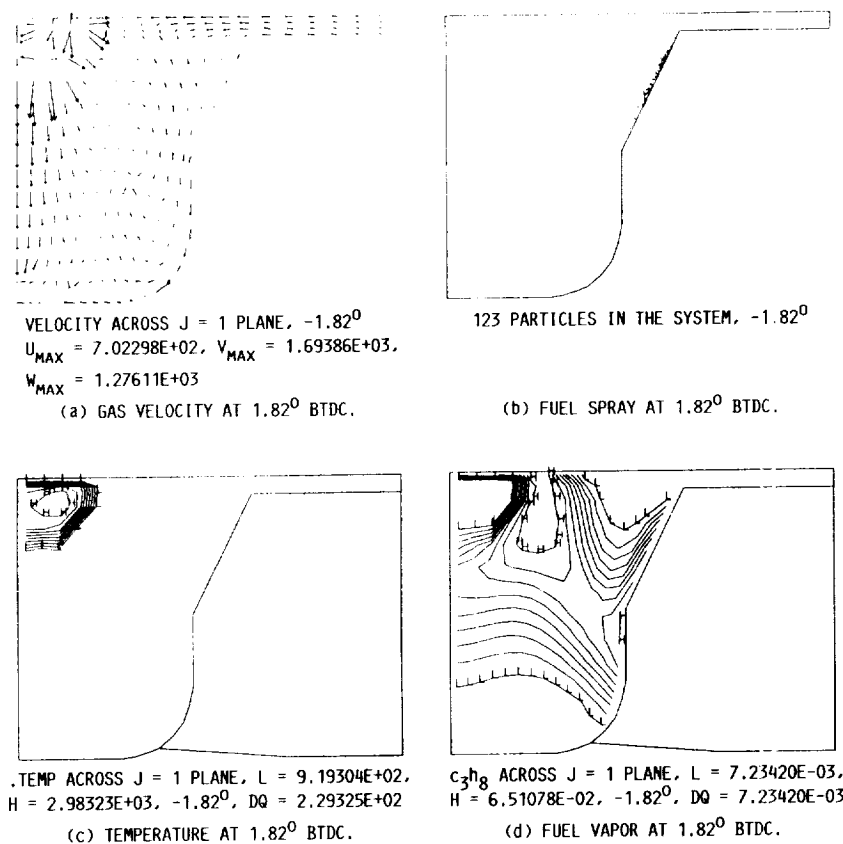
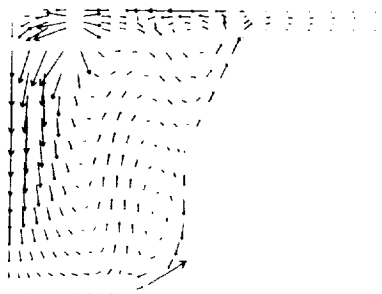
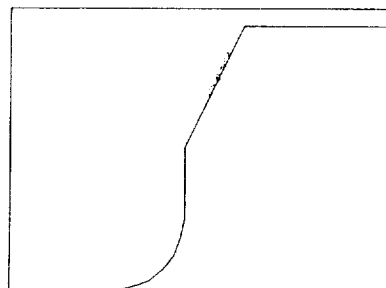


FIGURE 3. - RESULTS OF DISC GASOLINE-FUELED PISTON ENGINE FOR CASE 3.



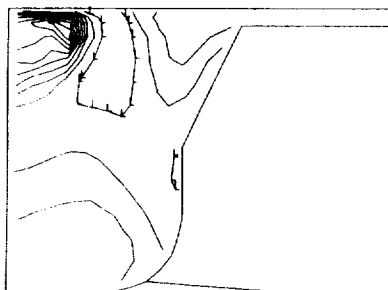
VELOCITY ACROSS J = 1 PLANE,  $-0.16^\circ$ ,  
 $U_{MAX} = 1.20566E+03$ ,  $V_{MAX} = 3.54255E+03$ ,  
 $W_{MAX} = 1.16764E+03$

(a) GAS VELOCITY AT  $0.16^\circ$  BTDC.



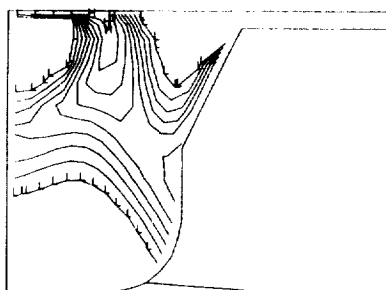
28 PARTICLES IN THE SYSTEM

(b) FUEL SPRAY AT  $0.16^\circ$  BTDC.



.TEMP ACROSS J = 1 PLANE,  $L = 9.71871E+02$ ,  
 $H = 2.62905E+03$ ,  $-0.16^\circ$ ,  $DQ = 1.65718E+02$

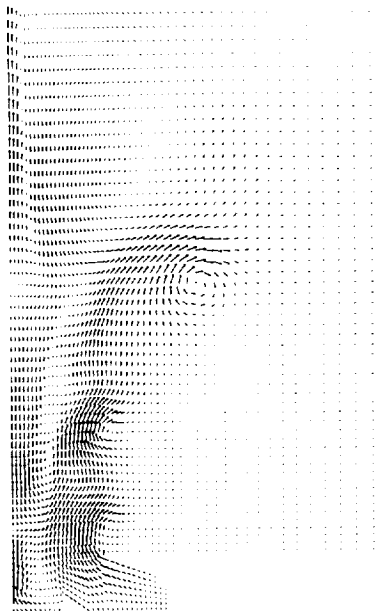
(c) TEMPERATURE AT  $0.16^\circ$  BTDC.



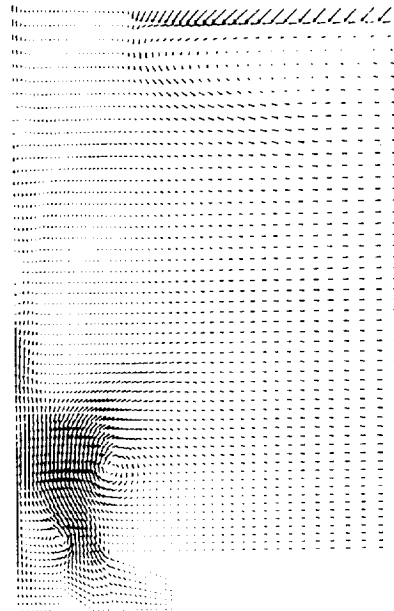
$C_3_8$  ACROSS J = 1 PLANE,  $L = 9.09029E-03$ ,  
 $H = 8.18126E-02$ ,  $-0.16^\circ$ ,  $DQ = 9.09029E-03$

(d) FUEL VAPOR AT  $0.16^\circ$  BTDC.

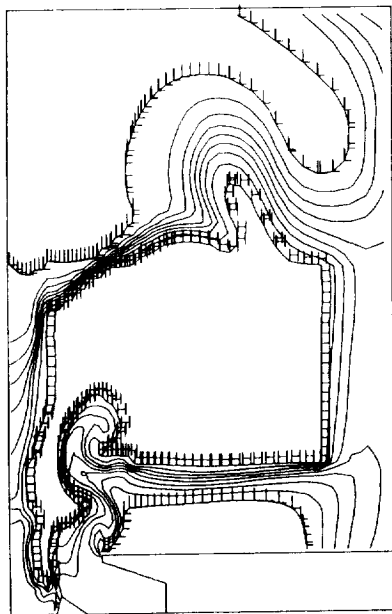
FIGURE 4. - RESULTS OF DISC GASOLINE-FUELED PISTON ENGINE FOR CASE 4.



VELOCITY ACROSS J = 1 PLANE,  
 $T = 8.26447\text{E-}03$ , CYCLE 1200,  
 $U_{\text{MAX}} = 1.20066\text{E}+04$ ,  $V_{\text{MAX}} = 1.21813\text{E}+04$ ,  
 $W_{\text{MAX}} = 1.73781\text{E}+04$

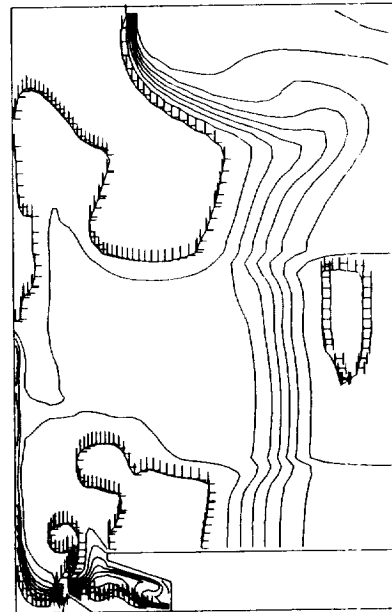


VELOCITY ACROSS J = 1 PLANE,  $T = 4.15503\text{E-}03$ ,  
 CYCLE 1200,  $U_{\text{MAX}} = 5.59223\text{E}+04$ ,  $V_{\text{MAX}} =$   
 $2.63656\text{E}+04$ ,  $W_{\text{MAX}} = 5.33020\text{E}+04$



TEMP ACROSS J = 1 PLANE,  $L = 1.07907\text{E}+03$ ,  
 $H = 1.58762\text{E}+03$ ,  $T = 8.26447\text{E-}03$ , CYCLE  
 1200, MIN =  $1.01551\text{E}+03$ , MAX =  $1.65119\text{E}+03$ ,  
 $DQ = 6.35683\text{E}+01$

(a) OCTANE COMBUSTION.



TEMP ACROSS J = 1 PLANE,  $L = 5.29182\text{E}+02$ ,  
 $H = 1.48754\text{E}+03$ ,  $T = 4.15503\text{E-}03$ , CYCLE  
 1200, MIN =  $4.09387\text{E}+02$ , MAX =  $1.60733\text{E}+03$ ,  
 $DQ = 1.19794\text{E}+02$

(b) PROPANE COMBUSTION.

FIGURE 5. - SIMULATION OF COMBUSTION IN TWO-DIMENSIONAL COMBUSTOR.

# Report Documentation Page

|  |  |  |   |   |  |
|--|--|--|---|---|--|
| 1. Report No.<br>NASA TM-103173<br>AIAA-90-2439  |  | 2. Government Accession No.                              |   | 3. Recipient's Catalog No.  |  |
| 4. Title and Subtitle<br><br>Critical Evaluation of Jet-A Spray Combustion Using Propane Chemical Kinetics in Gas Turbine Combustion Simulated by KIVA-II  |  |  |   | 5. Report Date  |  |
|  |  |  |   | 6. Performing Organization Code                                   |  |
| 7. Author(s)<br><br>H.L. Nguyen and S.-J. (Benjamin) Ying  |  |  |   | 8. Performing Organization Report No.<br><br>E-5551               |  |
|  |  |  |   | 10. Work Unit No.<br><br>537-01-11                                |  |
| 9. Performing Organization Name and Address<br><br>National Aeronautics and Space Administration<br>Lewis Research Center<br>Cleveland, Ohio 44135-3191  |  |  |   | 11. Contract or Grant No.   |  |
|  |  |  |   | 13. Type of Report and Period Covered<br><br>Technical Memorandum |  |
| 12. Sponsoring Agency Name and Address<br><br>National Aeronautics and Space Administration<br>Washington, D.C. 20546-0001   |  |  |   | 14. Sponsoring Agency Code  |  |
|  |  |  |   |   |  |
| 15. Supplementary Notes<br><br>Prepared for the 26th Joint Propulsion Conference cosponsored by the AIAA, SAE, ASME, and ASEE, Orlando, Florida, July 16-18, 1990. H.L. Nguyen, NASA Lewis Research Center, Cleveland, Ohio 44135; S.-J. (Benjamin) Ying, University of South Florida, Tampa, Florida 33620.   |  |  |   |   |  |
| 16. Abstract<br><br>Jet-A spray combustion has been evaluated in gas turbine combustion with the use of propane chemical kinetics as the first approximation for the chemical reactions. In this work, the numerical solutions are obtained by using the KIVA-II computer code. The KIVA-II code is the most developed of the available multidimensional combustion computer programs for application of the in-cylinder combustion dynamics of internal combustion engines. The released version of KIVA-II assumes that 12 chemical species are present; the code uses an Arrhenius kinetic-controlled combustion model governed by a four-step global chemical reaction and six equilibrium reactions. Our efforts involve the addition of Jet-A thermophysical properties and the implementation of detailed reaction mechanisms for propane oxidation. Three different detailed reaction mechanism models are considered. The first model consists of 131 reactions and 45 species. This is considered as the full mechanism which is developed through the study of chemical kinetics of propane combustion in an enclosed chamber. The full mechanism is evaluated by comparing calculated ignition delay times with available shock tube data. However, these detailed reactions occupy too much computer memory and CPU time for the computation. Therefore, it only serves as a benchmark case by which to evaluate other simplified models. Two possible simplified models have been tested in the existing computer code KIVA-II for the same conditions as used with the full mechanism. One model is obtained through a sensitivity analysis using LSENS, the general kinetics and sensitivity analysis program code of D.A. Bittker and K. Radhakrishnan. This model consists of 45 chemical reactions and 27 species. The other model is based on the work published by C.K. Westbrook and F.L. Dryer. |  |  |   |   |  |
| 17. Key Words (Suggested by Author(s))<br><br>Spray combustion<br>Gas turbine engine<br>Computational fluid dynamics   |  |  | 18. Distribution Statement<br><br>Unclassified - Unlimited<br>Subject Category 31 |   |  |
| 19. Security Classif. (of this report)<br><br>Unclassified   |  | 20. Security Classif. (of this page)<br><br>Unclassified |   | 21. No. of pages<br><br>20  |  |
|  |  |  |   | 22. Price*<br><br>A03   |  |